THE DOUBLE SCATTERING OF ^{3}He-PARTICLES BY CARBON AND ALUMINIUM

By W. E. Burcham, J. B. A. England and R. G. Harris

University of Birmingham*

and J. E. Evans†

A.E.R.E., Harwell**

(Received February 8, 1970)

Experiments on the double scattering of ^{3}He particles of energy near 30 MeV by carbon and aluminium targets are described. Observed polarizations are less than 0.1 in the centre of mass angular range 28°—35° in the most reliable experiments. Implications for the spin-orbit potential in ^{3}He-nucleus scattering are discussed.

1. Introduction

The elastic scattering of helium ions by nuclei has attracted the interest of physicists ever since the earliest experiments of Rutherford and his students. Already in these early experiments, which gave rise to the nuclear hypothesis, it was seen in the so-called anomalous scattering that the form and structure of the nucleus, as well as its existence, might be established. It is in this aspect especially that recent years have witnessed such great developments in alpha particle scattering work, as a result jointly of the availability of accelerator sources of particles and detectors of high resolution, and of the existence of the nuclear optical model as a suitable theoretical framework. At the time when Henryk Niewodniczański studied under Rutherford in the Cavendish Laboratory, the accelerators and detectors now shown to be desirable were not available, but interest in alpha scattering and transmutation processes was far from negligible. It was only to be expected then that this subject should engage Niewodniczański's personal attention as soon as the necessary facilities were afforded to him and alpha particle scattering was from the beginning a high priority in the Cracow Laboratory. The results of some of this

* Address: Department of Physics University of Birmingham, Birmingham 15, England.
** Address: A.E.R.E., Harwell, England.
† Deceased.

work, which are incidentally typical of those of several other laboratories working in this field, have been published [1]. It is characteristic of Niewodniczański's thoroughness that he was not content to confine the attention of his group to elastic scattering data, but sought also further to constrain the analysis by making quite difficult measurements of reaction cross sections.

The optical model analysis of alpha particle scattering was reviewed in 1963 by Hodgson [2]. In such analyses, the nuclear scattering potential is usually assumed to have a Saxon-Woods radial form, as is indicated, at least for the charge distribution in the heavier nuclei, by electron scattering work.

The connection between model parameters, such as well depth and charge and matter radii, and the properties of the nucleon-nucleon force has recently received much attention, especially for proton scattering [3]. For alpha particle scattering, a similar approach has also been made [4], with some success. An obvious difference between the results of the proton and alpha analysis is that, neglecting distortion of the incident alpha particle, effects due to the two-body spin-orbit potential cancel out in alpha scattering and there is no expectation of polarization effects. In the case of the light isotope of helium however spin effects should be apparent and observation of them may help in an understanding of the optical model analysis of complex particle scattering. The present work, which started in 1963, was the first attempt to estimate the magnitude of the phenomenological spin-orbit potential in ^{3}He-nucleus scattering.

2. *The optical model for ^{3}He-scattering*

The conventional formulation of the optical potential for ^{3}He scattering is discussed by Hodgson [5]. It expresses the potential as the sum of the constituent nucleon potentials averaged over the internal wavefunction of ^{3}He. The central potential is then about three times that for nucleons and the spin-orbit potential about one third, but it is pointed out that the potentials are best found by optimising fits to the experimental data. The potentials, however, may be expected to retain some of the features of the nucleon optical potential, such as a prediction [6] that polarization changes rapidly in the vicinity of a diffraction minimum in the elastic scattering. Since the diffraction peaks for ^{3}He-nucleus scattering are sharper and more closely spaced than those for scattering of nucleons of the same or lower energy, the determination of polarization is a more difficult problem than in the case of proton scattering, It was decided to make measurements at the highest available energy (30 MeV) with a nucleus (^{12}C, ^{27}Al) for which good elastic scattering data were available, and at an angle somewhat removed from the first diffraction minimum, so that the polarization, although less in magnitude, would also be less angle-dependent. Fig. 1 shows angular distributions for the scattering of 29 MeV ^{3}He ions by ^{12}C and the range of c.m. angles covered in the measurements. In all the experiments reported here the double scattering technique was employed. In this the polarization $P(\theta)$ produced by scattering in a first target at c.m. angle θ is assessed by observing the ratio ε of second scattering to the left and to the right by a similar target. If energy changes in the scattering are neglected, two scatterings in the same direction should always give a greater intensity than one scattering to the left

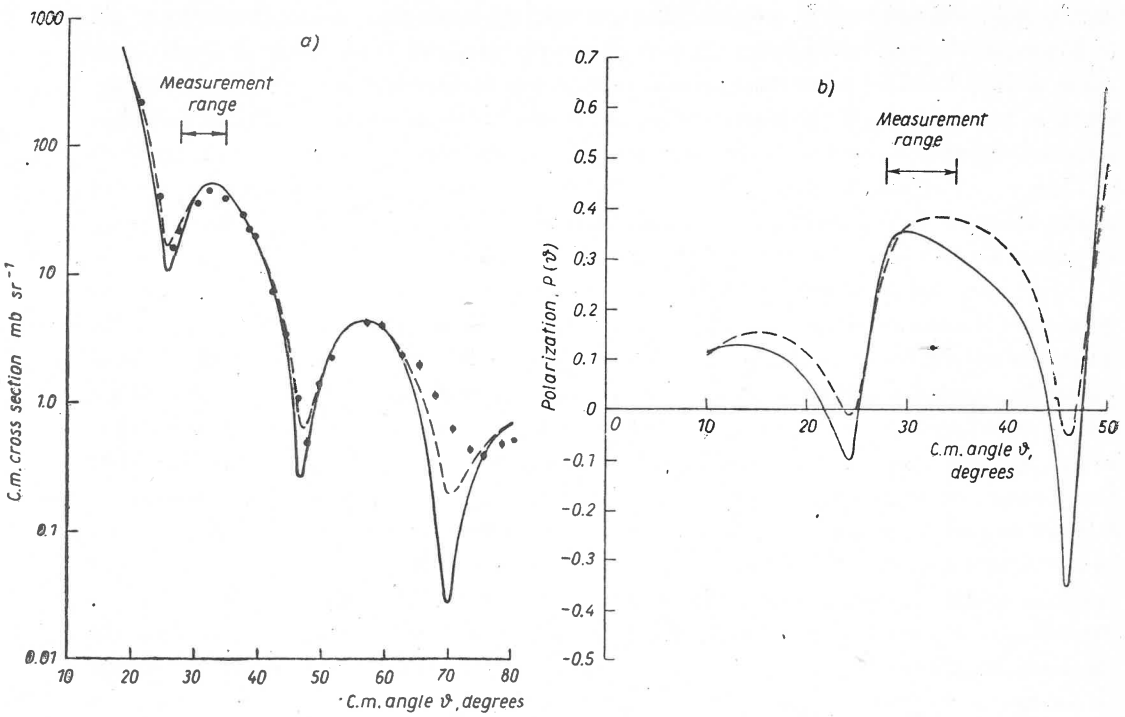

Fig. 1(*a*). Differential cross sections for the scattering of 29 MeV ^{3}He particles by ^{12}C. ● experimental points; — — — prediction using optical model parameters type 1 (Table III) for an energy 28.3 MeV; ——— prediction for parameters type 2. (*b*). Polarization predicted in the scattering of 28.3 MeV ^{3}He particles by ^{12}C with a 15 MeV spin-orbit potential. — — — parameters type 1; ——— parameters type 2

and one to the right and ε can therefore be defined to be greater than or equal to unity. Under these circumstances the asymmetry

$$\Sigma = \frac{\varepsilon - 1}{\varepsilon + 1}$$

is also positive and equal to $[P(\theta)]^2$.

3. Experimental arrangement

3.1. Nuclear emulsion experiments

The first experiments were made using a 30 cm scattering chamber at the centre of which was supported a carbon foil of thickness equivalent to 2.45 mgm cm^{-2} to act as the first scattering target. The ^{3}He beam of the Nuffield cyclotron was collimated to a diameter of about 6 mm and passed through the first target to a distant Faraday cup; beams of up to 10 μA were used.

Particles scattered from the first target were received by a second foil mounted behind collimators on a small carriage which could move through an angular range of ±35° about a vertical axis intersecting the first target. The second scattering foil was of carbon (3.3 mgm

cm^{-2}), gold (48 mgm cm^{-2}), copper (22 mgm cm^{-2}), aluminium (5.4 mgm cm^{-2}), or tin (6.8 mgm cm^{-2}), and could intercept particles scattered down from the first target at an angle of 15°. Particles scattered a second time within an angular range ±50° horizontally could be received in a photographic emulsion mounted on the movable carriage. This then acted as a detector of any left-right asymmetry in the second scattered beam. After an exposure yielding a convenient track density in the emulsion, the plate was processed and counts of tracks of length corresponding to elastically scattered ^{3}He particles were made over a range of angles on the plate for a first scattering angle within the range 28–33° (lab.).

For a first target of carbon and a second target of gold, little asymmetry was expected because of the mainly Coulomb interaction of 26 MeV ^{3}He ions with a nucleus with $Z = 79$. The experimental results for these exposures have already been published [7] and show a well-defined second-scattered peak but with a near-zero asymmetry. Plates taken with carbon as first target, and carbon, aluminium, copper and tin as second target were next scanned in the hope that asymmetries would be observable. Effects were indeed found [8, 9] but were considered to be subject to systematic error because of the effect of (^{3}He, α) reactions in both targets. In the case of the gold analyser, the effect of contamination α-particles and of recoil protons from neutron background could be reasonably well estimated relative to the large elastic ^{3}He peak. With a carbon analyser however and with no mass discrimination available, this proved very difficult. Moreover, the geometrical definition of the nuclear emulsion experiment was less precise than desirable. It was therefore decided (May 1963) to set up an electronic system using counter telescopes.

3.2. Counter telescope experiments

3.2.1. General arrangement

In replacing the nuclear emulsion plate by counter telescopes, with a well-defined acceptance angle, it was necessary to make a careful choice of first and second scattering angles. For the ^{3}He—^{12}C elastic scattering the data available at 23–32 MeV in 1964 [10–12] had been taken at 5° intervals (c. m.) with an angular resolution of about ½°. Optical model analyses [13] had shown that differential cross section data of this quality were not very sensitive to the magnitude of spin-orbit terms in the optical potential, and that the polarization (using a 15 MeV spin orbit term) would vary as shown in Fig. 1[1]. A flat maximum in the polarization appeared at an angle corresponding to 27° (lab) and this was chosen for the first experiments.

Fig. 2 shows the experimental arrangement adopted for the counter telescope experiments. Inside the 30 cm diameter chamber was a precisely machined wedge-shaped carriage which could be rotated about the first target, T_1, through angles of up to 30° on either side of the main beam line. This carriage was fitted with a second target, T_2, at a distance of 9 cm from the first target. The second target could be changed remotely from carbon to gold in order to check the geometrical asymmetries of the carriage at each setting.

Semiconductor counters of the silicon-surface barrier type were arranged to form two $E-\Delta E$ counter telescopes. The ΔE counters were of thickness corresponding to a ^{3}He energy loss of 4 MeV and the E counters were sufficiently thick to stop ^{3}He particles passing

[1] Later calculations by Frahn and Wiechers [14] using a strong absorption model yielded similar results.

through the ΔE detectors. The counter telescopes were mounted on accurately made collimating stops, $S3$, at distance of 8 cm from the second target (Fig. 2). Each counter assembly could be rotated about the second target through angles from 17°–30° with the first scattered beam line.

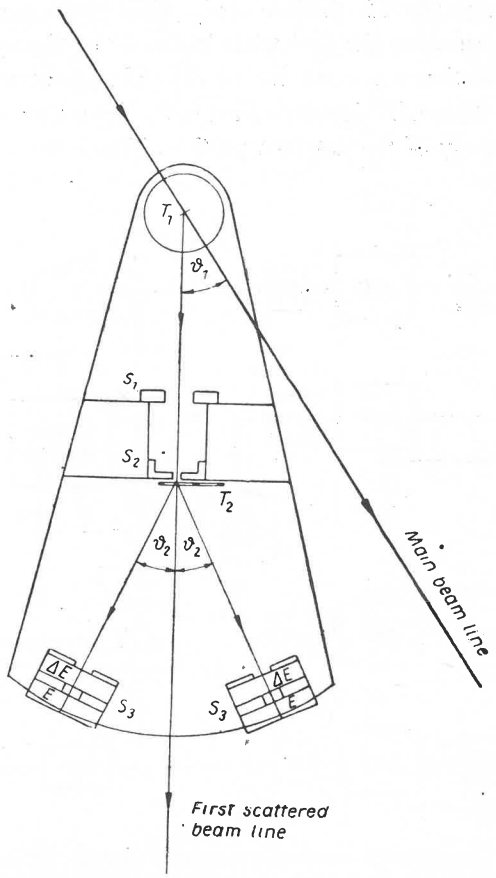

Fig. 2. Experimental arrangement of wedge polarimeter for counter telescope double scattering experiments The stop dimensions are: $S1$ 14.5 mm × 9.5 mm tantalum; $S2$ 9.5 mm × 2.4 mm carbon; $S3$ 9.5 mm × 6.35 mm dural

The angular definition of the main beam on to the first target was $\pm\frac{1}{2}°$. In addition, in order to reduce the possibility of beam wander, a strip first target T_1 of width 3 mm was used. The scattered beam was collimated by two rectangular apertures $S1$ and $S2$. The angular spread in the scattered beam from the first target on to the second was about $\pm 1°$. The counter collimating stops $S3$ had an angular acceptance of $\pm 2°$.

In the first experiments with a first scattering angle of 27° the counter telescopes were arranged symmetrically at 27° on either side of the first scattered beam line. The particle identification function of the counter telescopes was tested with a system developed by Lowe [15] based on an oscilloscope display of the combined deflection produced by signals

in the x and y directions which were proportional to the pulse-heights of the E and ΔE counter pulses respectively. Distinct traces corresponding to the ^{3}He and ^{4}He particles were seen confirming the mass separation. In making asymmetry measurements, a mask on the face of the oscilloscope was arranged to obscure the ^{4}He trace from a photomultiplier tube which gated the electronic system for ^{3}He particles only. This cumbersome system was subject to drift and was abandoned after the first trials in favour of the system shown in Fig. 3 which with some modification was used for all the subsequent work.

As indicated in Fig. 3, the ΔE signal is added to the E counter signal to produce a pulse representing the total energy of the detected particle. This is multiplied by the ΔE signal

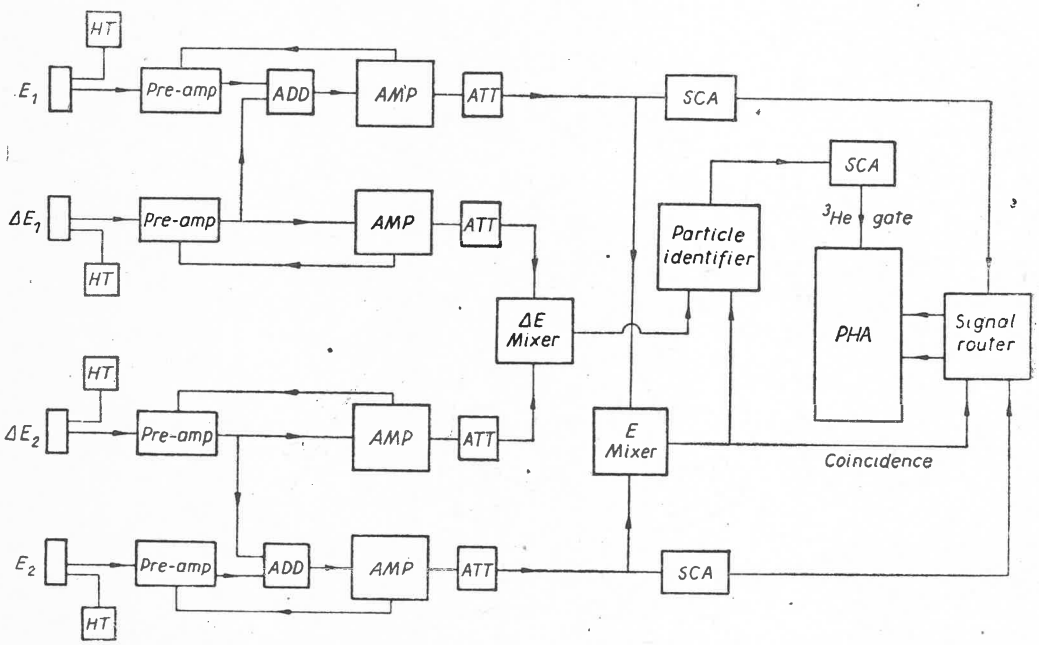

Fig. 3. Electronic circuit for counter telescope double scattering experiments, showing pulse height anlysaer (*PHA*), single channel analyser (*SCA*), pulse adding circuit (*ADD*) and fine attenuator (*ATT*)

itself to obtain an output proportional to MZ^2 where M is the mass of the particle and Z its charge. The mass peaks for ^{3}He and ^{4}He should therefore stand in the ratio 3 to 4 in pulse size, although the actual separation will depend on the performance of the counters and the pulse multiplying circuit [16] used. Fig. 4 shows the discrimination achieved in the later stages of this work. If now the telescope output is only accepted when the MZ^2 signal corresponds to a selected range of pulses within the mass 3 peak, ^{3}He particles are selected with high efficiency. Fig. 5 shows telescope spectra recorded by the pulse analyser when both the first and second targets were carbon foils, The effect of MZ^2 gating in removing the α-particle peaks due to the ^{12}C(^{3}He, ^{4}He)^{11}C reaction in the targets is clearly seen.

The first carbon-carbon measurement made with this apparatus gave a result which seemed to agree with the photographic plate measurements, and has already been reported [8].

Small asymmetry was found in the C—Au scattering; essentially no mass-gated counts were obtained when either the first or second target was removed. Slit scattering effects were minimised by the use of carbon collimating apertures on the wedge (Fig. 2).

The first observations were made with the analyser wedge on one side of the primary beam only. Before these measurements could be extended to the other side, trouble developed with the cyclotron and with the counters, whose performance deteriorated because of radia-

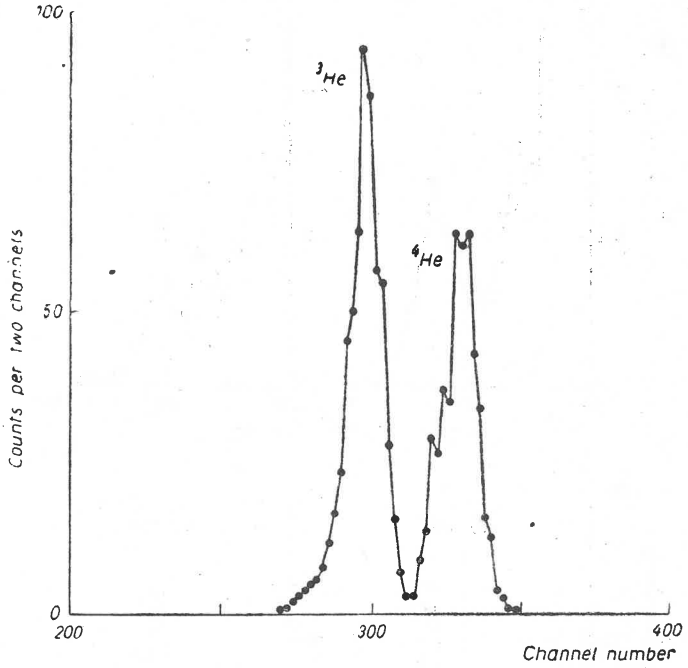

Fig. 4. Output ($\propto MZ^2$) of pulse multiplier circuit showing discrimination between ^{3}He and ^{4}He peaks from carbon second target with ^{3}He particles incident on the carbon first target ($\vartheta_1 = \vartheta_2 = 25°$lab)

tion damage and contamination by cracked hydrocarbon vacuum pump oil. On resuming the experiments and checking the C—C asymmetry at laboratory angles of 27° only a small (negative) asymmetry was found. When the results for the four polarimeter wedge positions were averaged the C—Au asymmetry was effectively zero as before. As pointed out in Sec. 2 the asymmetry should be positive in an ideal experiment and equal to $[P(\theta)]^2$. Negative asymmetries could arise because of a sharp variation of $P(\theta)$ with energy but this seemed unlikely (see, for instance, Fig. 8). The origin of the negative asymmetry was therefore felt to be either statistical or instrumental, and to eliminate the latter possibility the electronic and geometrical conditions of the whole experiment were carefully examined.

3.2.2. Electronics errors

The performance of the pulse multiplier and routing system were exhaustively checked and shown to be reliable. Particular attention was paid to the possible dependence of the multiplier output on particle energy and to the possibility of random routing of pulses.

An additional check that variations in asymmetry were not due to the multiplier was obtained from results with aluminium first and second targets. In this case the yield of reaction α-particles is much less than with carbon and the multiplier could be eliminated; despite this, variations in asymmetry were still observed.

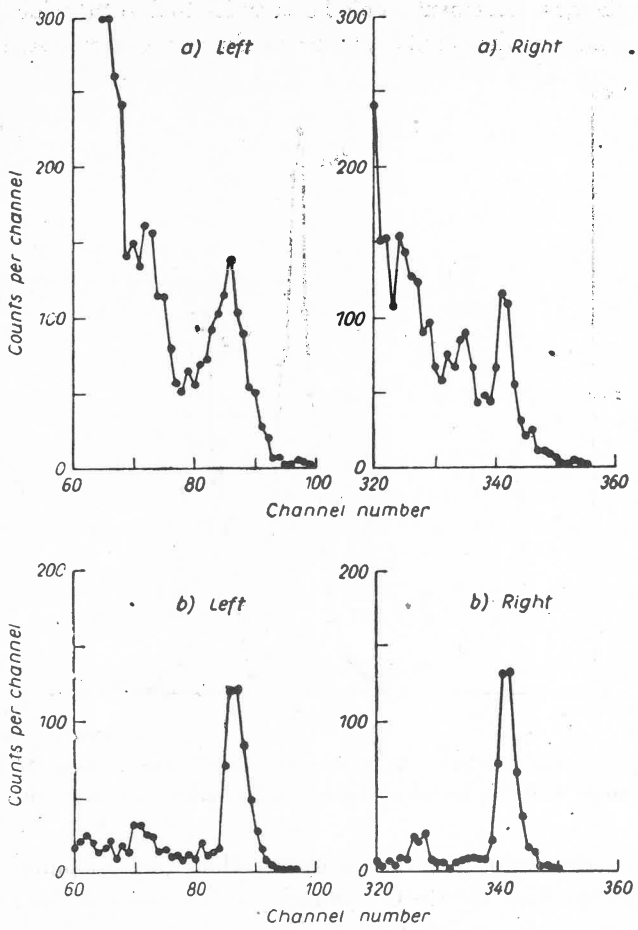

Fig. 5. Effect of MZ^2 gating on pulse height spectra of particles from second target under conditions as specified for Fig. 4. Peaks for both left and right counter telescopes are shown, (*a*) No gating, (*b*) Gating; ^{4}He peaks arising from the $^{12}C(^3He, \alpha)$ reaction are eliminated

The counter performance was improved by fitting liquid air traps close to the scattering chamber. When all possible care had been taken with counters, amplifiers and pulse analyser, the necessary long term stability of 1% in gain over 24 hours was achieved.

3.2.3. Geometrical errors

An obvious source of variation in the observed asymmetries is lack of geometrical precision. It had been hoped that with a definition of angles to 2° or less it would be possible to correct reliably for any asymmetry of the wedge polarimeter by replacing the carbon

(or aluminium) second target by gold and taking the ratio of the asymmetry in the two cases for the same first target. This procedure, which was in the end used in the analysis, does not correct fully for effects due to beam wander on the first target because of the different variation of differen al cross section with angle for the two second targets. With a carbon--carbon arrangement the ratio of left to right telescope counts could be varied from 0.7 to 1.3 by moving the beam laterally on a wide first target but only about a third of this variation was seen with a gold second target. Restriction of the first target width to 3 mm reduced but did not eliminate this effect. Rapid scanning of the beam across the first target also gave some improvement and was used in many of the runs, but the effect was never entirely removed. The use of a composite second target made by evaporating a thin film of gold on to the surface of an aluminium foil so that (under conditions of good energy resolution) aluminium-aluminium and aluminium-gold observations could be taken simultaneously was also nusuccessful in achieving good reproducibility. It was concluded that the experiment was being limited by asymmetry changes arising from angular variations of the order of $^1/_3°$; calculations based on the best available cross section data confirmed that such variations could be important if beam wander took place.

A further geometrical error of a more subtle character was found to be a slight lack of reproducibility of the distance between the first target and the axis of rotation of the polarimeter wedge. This was found during experiments in which asymmetries for aluminium--aluminium and aluminium-gold were observed in succession for the four possible positions

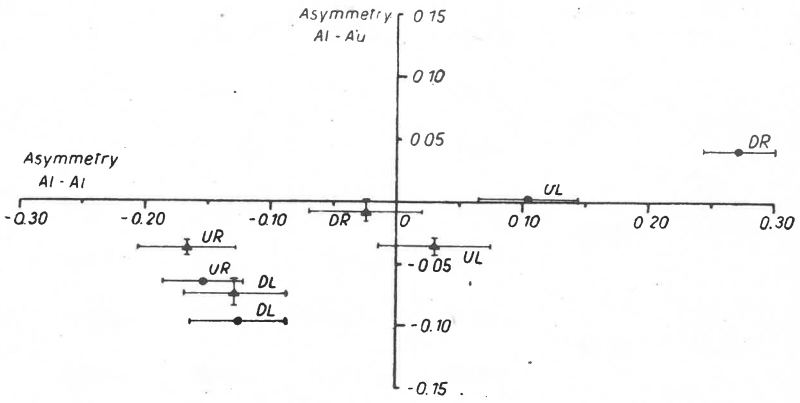

Fig. 6. Asymmetries observed in successive runs with the arrangements Al—Al, and Al—Au for four polarimeter positions and two angles. The scatter of the points is ascribed to small changes of first to second target distance on polarimeter inversion. The wedge positions are indicated as *UL* (up-left), *UR* (up-right), *DL* (down-left) *DR* (down-right). ● —23° lab. results, ▲ —25° lab. results

of the polarimeter wedge (up-left, down-left, up-right and down-right). If the asymmetry for Al—Al is plotted against that for Al—Au the resulting points should all be in one quadrant of the diagram (Fig. 6). In fact the points scatter between three quadrants; the observed distribution is consistent with the effect of a change of about 1.5 mm in the distance between first target and second target on polarimeter inversion. Change of the polarimeter

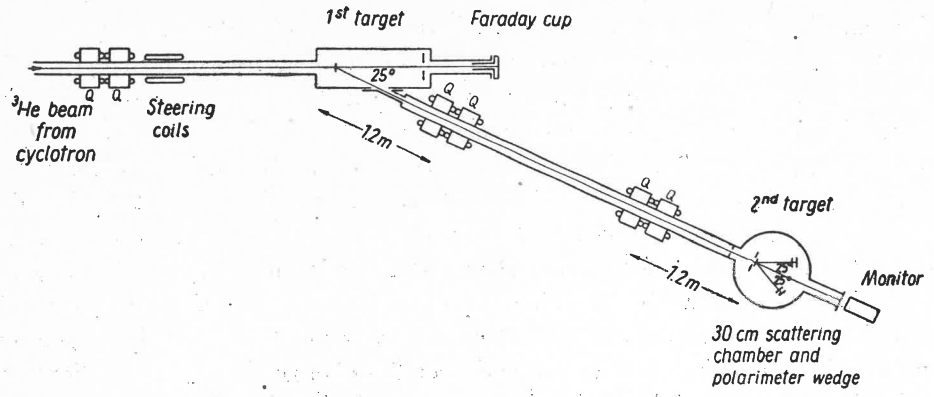

Fig. 7. Quadrupole-focussed first scattered beam used in final double scattering experiments. The second scattered particles are detected in the counter telescopes of the polarimeter wedge

TABLE I

Experimental results for double scattering of 30 MeV ^{3}He particles by carbon

Dates of runs	Scattering angle θ First	Second	C—Au $(\varepsilon)^1$	C—C $(\varepsilon)_{raw}$	C—C $(\varepsilon)_{norm}$	Asymmetry $\Sigma_{norm.}$	Limits of $P(\theta)$
14.9.64 to 18.9.64	27°lab	27°lab	0.980 ±0.020	0.942 ±0.040	0.961 ±0.039	−0.017 ±0.020	0.0 to 0.055
7.2.65 to 16.2.65	23°lab	23°lab	1.025 ±0.011	1.049 ±0.031	1.023 ±0.037	+0.012 ±0.019	+0.065 to −0.110
16.2.65 to 22.2.65	25°lab	25°lab	1.018 ±0.016	1.010 ±0.047	0.993 ±0.048	−0.004 ±0.024	0.0 to 0.142
22.2.65 to 25.2.65	27°lab	23°lab	0.917 ±0.015	1.049 ±0.052	1.145 ±0.056	+0.068 ±0.023	
25.2.65 to 28.2.65	25°lab	23°lab	0.998 ±0.009	1.065 ±0.055	1.065 ±0.056	+0.031 ±0.027	
17.3.65 to 31.3.65.	27°lab	27°lab	0.980 ±0.023	0.968 ±0.044	0.988 ±0.052	−0.006 ±0.027	0.0 to 0.145

[1] (ε) is the averaged ratio of the number of particles scattered in the same sense at the second scatterer relative to the first scatterer over the number of particles scattered in the opposite sense at the second scatterer relative to the first scatterer.

TABLE II

Experimental results for double scattering of 30 MeV ^{3}He particles by aluminium

Dates of runs	Scattering angle θ First	Second	Al—Au (ε)[1]	Al—Al $(\varepsilon)_{raw}$	Al—Al $(\varepsilon)_{norm}$	Asymmetry Σ_{norm}	Limits of $P(\theta)$
20.8.65 to 29.8.65	23°lab	23°lab	0.942 ±0.010	1.051 ±0.050	1.115 ±0.055	+0.056 ±0.022	+0.04 0.24 −0.06
29.8.65 to 3.9.65	25°lab	25°lab	0.926 ±0.020	0.869 ±0.072	0.938 ±0.088	−0.032 ±0.046	0.0 to 0.1
10.12.65 to 13.12.65[2]	25°lab	25°lab	0.960 ±0.025	0.968 ±0.090	1.009 ±0.093	+0.005 ±0.043	+0.15 0.07 −0.07
16.12.65 to 17.12.65[2]	25°lab	25°lab	0.907 ±0.065	0.910 ±0.050	1.003 ±0.080	+0.002 ±0.042	+0.200 0.045 −0.045

[1] (ε) is the averaged ratio of the number of particles scattered in the same sense at the second scatterer relative to the first scatterer over the number of particles scattered in the opposite sense at the second scatterer relative to the first scatterer.

[2] Results taken with the extended beam line shown in Fig. 7.

to the other side of the primary beam, without inversion, produced a similar but smaller shift.

The solution to both geometrical problems was to increase the first to second target distance so that the effects of angular errors and of longitudinal displacements were minimised. The distance was increased from 90 mm to 4 m and in order to preserve the same solid angle a quadrupole magnet system was used to focus the first scattered beam on to the second target (Fig. 7). Rotation of polarization due to passage of the first scattered beam through the quadrupoles was estimated to be 4.5° at each quadrupole doublet, giving a negligible depolarization.

3.2.4 Polarimeter errors

The possibility of serious malfunction of the polarimeter wedge was investigated by using it to determine the asymmetry in the scattering of fully polarized protons by carbon. A beam of protons of energy 10.7 MeV and polarization $P = 1$ was obtained by recoil from the collisions of alpha particles in a hydrogen gas target. These protons passed through foils which reduced their energy to 6.8 MeV and were then incident on the second carbon target, in the polarimeter wedge. Reproducible asymmetries of 0.44 ± 0.04 were obtained without difficulty (and 0.004 with a gold scattering foil) compared with a value of 0.42 ± 0.03 previously measured [17].

4. *Results*

4.1. Counting rates

In typical experiments of this series, ^{3}He beam currents of up to 10 μA were used on the first target. The counting rate in the polarimeter telescopes was then about 0.3 counts per minute in the elastic ^{3}He peak for the C—C sequence at first and second scattering angles of 27° (lab.). For C—Au, the rate was 20 counts per minute. Observations were taken with various combinations of C, Al and Au targets at angles between 23° and 27° lab.

4.2. Method of analysis

In Sec. 2 a quantity ε was defined as the ratio of the number of particles scattered in the same sense at the second target as at the first, to the number scattered in the opposite sense at the second target. For given scattering angles there are four polarimeter positions (1–4) which have been described in Sec. 3 as up-left, down-left *etc.* If the four ε values for the sequence carbon-gold are averaged geometrically we obtain a quantity (ε) given by

$$(\varepsilon) = [\varepsilon_1(\mathrm{C{-}Au}) \times \varepsilon_2(\mathrm{C{-}Au}) \times \varepsilon_3(\mathrm{C{-}Au}) \times \varepsilon_4(\mathrm{C{-}Au})]^{1/4}$$

in which certain geometrical asymmetries such as counter apertures should cancel out. Similarly for the sequence C—C we may form the quantity

$$(\varepsilon)_{\mathrm{raw}} = [\varepsilon_1(\mathrm{C{-}C}) \times \varepsilon_2(\mathrm{C{-}C}) \times \varepsilon_3(\mathrm{C{-}C}) \times \varepsilon_4(\mathrm{C{-}C})]^{1/4}$$

We have assumed that the best correction of the carbon data by the observations with gold is effected by calculating the ratio

$$(\varepsilon)_{\mathrm{norm}} = \frac{(\varepsilon)_{\mathrm{raw}}}{(\varepsilon)}$$

and from this the asymmetry is finally derived as

$$\Sigma_{\mathrm{norm}} = \frac{(\varepsilon)_{\mathrm{norm}}^{\prime} - 1}{(\varepsilon)_{\mathrm{norm}} + 1}.$$

If the first and second scattering angles are equal and if the polarization changes little with energy over the energy range of two scatterings, this is equal to $[P(\theta)]^2$. If the first and second scattering angles are θ_1 and $\theta_2 (\neq \theta_1)$ then

$$\Sigma_{\mathrm{norm}} = P_1(\theta_1) \times P_2(\theta_2).$$

Table I gives values of (ε), $(\varepsilon)_{\mathrm{raw}}$ and $(\varepsilon)_{\mathrm{norm}}$ for scattering of ^{3}He by carbon deduced from observations at the indicated scattering angles. The errors shown in the table are the weighted statistical values obtained from the numbers of counts recorded in each elastic peak. Column 7 of Table I gives Σ_{norm} and column 8 the limits within which $P(\theta)$ may

be inferred to lie.[2] An energy at the first target of 30 MeV corresponds in this case to an energy of 28.3 MeV at the second target and the approximation of equal polarization for these two energies is seen from Fig. 8 to be valid for the angles used. In the cases tabulated where $\theta_1 \neq \theta_2$ it was felt that neither $P_1(\theta_1)$ nor $P_2(\theta_2)$ was sufficiently well established to allow calculation of the other.

Table II gives similar results for the scattering of ^{3}He by aluminium. Again the approximation $\Sigma_{1\,\mathrm{norm}} = [P(\theta)]^2$ has been used, and although this has not been checked specifically it is expected to be valid because the elastic scattering angular distribution is a slowly varying function of energy near 30 MeV. The data at 23° (20.8/65) and 25° (29.8.65) were taken using the geometrical arrangement also employed for the carbon data (Table I and Sec. 3.2.1.). The data at 25° (10.12.65) were taken with the extended beam line (Fig. 7) and for the 25° data (16.12.65) the extended beam line and the composite target (Sec. 3.2.3.) were used. It is felt that the three sets of results for ^{3}He scattering by aluminium at 25° are the most reliable of the whole series and that the spread seen in these is typical of what can be expected. It seems clear that at the angles studied the polarization for both carbon and aluminium is very small. This is in agreement with carbon double scattering results obtained in other laboratoratories [18] and with observations on first-scattered beams using a hydrogenous polarimeter [19].

5. *Optical model predictions of* ^{3}He-^{12}C *spin-orbit potential*

Angular distributions for the elastic scattering of ^{3}He particles by ^{12}C (Fig. 1*a*) were first analysed using a four parameter optical model with a potential of the form

$$V(r) = V_c(r) - (U + iW) f(r)$$

the form-factor $f(r)$ being of Saxon-Woods type. The polarization prediction shown in Fig. 1*b* was obtained by Hodgson [13] by inclusion of a spin-orbit term of the form

$$V_{SO}(r) = \left(\frac{\hbar}{\mu c}\right)^2 \frac{U_{SO}}{r} \frac{d}{dr} [f(r)]\, \sigma \cdot l$$

with U_{SO} taken to be 10–15 MeV. This potential gave an acceptable fit to the available elastic scattering data for 28.3 and 29 MeV ^{3}He particles with the parameters shown in TableIII (*cf.* Fig. 1). In the c.m. angular range 28°–40° the polarization ranges from 0.4 to 0.2 without sharp variation; this angular range includes the laboratory angles used in the present experiment.

Hutson *et al.* [18] obtained quite different polarization predictions using parameters derived from their analysis of 36 and 42 MeV elastic scattering data. Since the effect of the spin-orbit term is only second order in the differential cross section a fairly wide range of spin-orbit potentials can be used which produce only small differences in the fit to the angular distribution. Fig. 8 shows the predicted polarization for three values of U_{SO} using the parameters of Hutson *et al.* [18] with incident ^{3}He energies of 31.6 and 28.3 MeV; the

[2] All experimental results are given for laboratory angles θ.

parameters are shown in Table III. As is seen from these predictions the polarizations obtained from the more recent parameters are very much smaller than those obtained from the earlier four-parameter basic optical model. The magnitude of the spin-orbit potential is not yet well established from the carbon double scattering experiments. If the present results are taken together with those of other workers [18] and the parameters of Hutson *et al.* (Table III) are used, a potential of 6^{+4}_{-2} MeV may be inferred for an energy of 31.6 MeV. This is in agreement with the value $\leqslant 5$ MeV indicated by the experiments with a hydrogeneous polarimeter [19]. It may be compared with the work of Patterson and Cramer [20] who deduce $U_{SO} = 2.7 \pm 0.7$ MeV at 22.5 MeV from spin-flip measurements in ^{3}He—^{12}C inelastic scattering. Luetzelschwab and Hafele [21] from an optical model analysis of the

TABLE III

Optical model parameters for ^{3}He-carbon interaction used for polarization predictions

Type[1]	^{3}He energy in MeV	U in MeV	r_u in fm	a_u in fm	W_v in MeV	W_s in MeV	r_w in fm	a_w in fm	U_{so} in MeV	r_s in fm	a_s in fm
1	28.3	50	1.6	0.6	60	0	1.6	0.6	15	1.6	0.6
2	28.3	66.7	1.6	0.59	52.4	0	1.6	0.59	15	1.6	0.59
3	28.3	127.1	1.03	0.87	2.34	11.5	1.38	0.85	(1) (3) (5)	1.14	0.69
4	31.6	127.1	1.03	0.87	2.34	11.5	1.38	0.85	(1) (3) (5)	1.14	0.69

[1] Potentials 1 and 2 are those of Hodgson (Ref. [13]); potentials 3 and 4 are those of Hutson *et al.* (Ref. [18])

elastic scattering of 30–35 MeV ^{3}He particles by ^{27}Al, ^{51}V, ^{59}Co and ^{60}Ni concluded that a spin-orbit potential of 2–5 MeV was required. Zurmühle and Fou [22] introduced spin-orbit potentials of 6 and 8 MeV to describe the elastic scattering of 15 MeV ^{3}He particles by ^{13}C and ^{48}Ca, but these were not necessarily optimum values. Fujisawa *et al.* [23] give a full discussion of the derivation of U_{SO} from analysis of ^{3}He elastic scattering on ^{58}Ni at an energy of 34.14 MeV. They conclude that U_{SO} depends upon the real potential assumed in the optical analyses and that values of $\leqslant 3$ MeV are probably required. Full references to similar work, including theoretical predictions of U_{SO}, are given by these authors. Potentials U_{SO} between 5 and 8 MeV have been used by Stock *et al.* [24] in their DWBA analysis of the Cr(^{3}He, α) reactions for $E_{\mathrm{He}} = 18$ MeV.

The small values of the spin-orbit potential indicated in this and other work are not inconsistent with the theoretical prediction [5, 18] that this potential should be of the order of one third of the spin orbit potential in the case of the nucleon-nucleus scattering. The

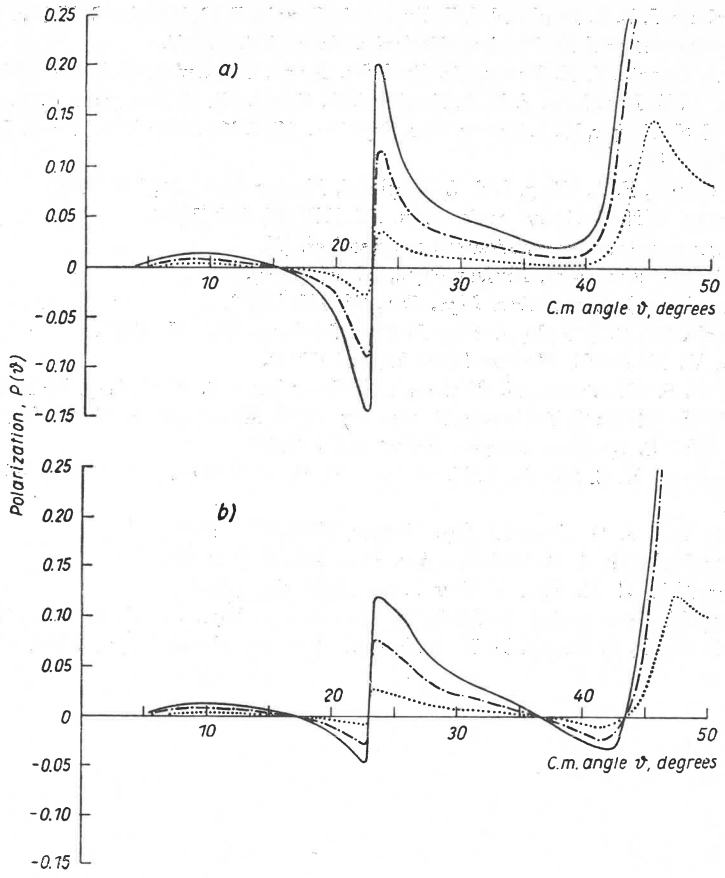

Fig. 8. Polarizations in $^{3}He-^{12}C$ scattering at (*a*) 31.6 and (*b*) 28.3 MeV using parameters from Hutson *et al.* [18] as shown in Table III. ——— $U_{so} = 5$ MeV; —·— 3 MeV; .... 1 MeV

resulting reduction in expected polarization to about 10% of that found with nucleons of comparable momenta is certainly enough to account for the variability of results encountered in the present series of experiments.

REFERENCES

[1] A. Budzanowski, K. Grotowski, J. Kuźmiński, H. Niewodniczański, A. Strzałkowski, S. Sykutowski, J. Szmider and R. Wolski, *Nuclear Phys.*, **A106**, 21 (1968).
[2] P. E. Hodgson, *The Optical Model of Elastic Scattering*, The Clarendon Press, Oxford 1963.
[3] G. W. Greenlees, G. J. Pyle and Y. C. Tang, *Phys. Rev.*, **171**, 1115 (1968).
[4] D. F. Jackson, C. G. Morgan, *Phys. Rev.*, **175**, 1402 (1968); D. F. Jackson, V. K. Khembavi, *Phys. Rev.*, **178**, 1626 (1969); C. G. Morgan, D. F. Jackson, *Phys. Rev.*, to be published.
[5] P. E. Hodgson, *Advances in Phys.*, **17**, 563 (1968).
[6] A. de Shalit, *Preludes in Theoretical Physics*, North Holland Publishing Co. P.O. Box 103, Amsterdam 1966, p. 35.
[7] J. Catala, A. Garcia, J. M. Perez, *An. Real Soc. Espan. Fiz. Quim.*, **61A**, 357 (1965).

[8] W. E. Burcham, J. B. A. England, J. E. Evans, A. Garcia, R. G. Harris, C. Wilne, *Comptes Rendus du Congres International de Physique Nucleaire*, Paris 1964, p. 877.
[9] J. Catala, A. Garcia, J. M. Perez, *An Real Soc. Espan. Fiz. Quim.*, **61A**, 357 (1965).
[10] J. Aguilar, W. E. Burcham, J. B. A. England, A. Garcia, P. E. Hodgson, P. V. March, J. S. C. McKee, E. M. Mosinger, W. T. Toner, *Proc. Roy. Soc.*, **A257**, 13 (1960); S. M. Morsy, *Thesis*, University of Birmingham 1963.
[11] H. M. Sen Gupta, E. A. King, J. B. A. England, *Nuclear Phys.*, **50**, 549 (1964).
[12] V. Pankratov, I. N. Serikov, *Soviet Phys. J.E.T.P.*, **17**, 604 (1963).
[13] P. E. Hodgson, private communication; see also Ref. [5].
[14] W. E. Frahn, G. Wiechers, *Nuclear Phys.*, **74**, 65 (1965).
[15] G. W. Greenlees, J. Lowe, *Proc. Phys. Soc.*, **76**, 149 (1960).
[16] J. H. Broadhurst, G. J. Pyle, *Nuclear Instrum. Methods.*, **48**, 117 (1967).
[17] S. J. Moss, W. Haeberli, *Nuclear Phys.*, **72**, 417 (1965).
[18] R. L. Hutson, S. Hayakawa, M. Chabre, J. J. Kraushaar, B. W. Ridley, E. T. Boschitz, *Phys. Letters*, **27B**, 153 (1968); T. Fujisawa, H. Kamitsubo, S. Motonaga, H. Matsuda , H. Sakaguchi, K. Masui, *I.P.C.R. Cyclotron Progress Report*, **2**, 77 (1968).
[19] J. B. A. England, R. G. Harris, L. H. Watson, D. H. Worledge, J. E. Evans, *Phys. Letters*, **30B**, 476 (1969).
[20] D. M. Patterson, J. G. Cramer, *Phys. Letters*, **27B**, 373 (1968).
[21] J. W. Luetzelschwab, J. C. Hafele, *Phys. Rev.*, **180**, 1023 (1969).
[22] R. W. Zurmühle, C. M. Fou, *Nuclear Phys.*, **A129**, 502 (1969).
[23] T. Fujisawa, H. Kamitsubo, T. Wada, M. Igarashi, *J. Phys. Soc. Japan*, **27**, 278 (1969).
[24] R. Stock, R. Bock, P. David, H. H. Duhm, T. Tamura, *Nuclear Phys.*, **A104**, 136 (1967).